

# UC Santa Barbara

## UC Santa Barbara Electronic Theses and Dissertations

### Title

Photomanipulation of Stress Relaxation in Alginate Hydrogels via Addition of PEG

### Permalink

<https://escholarship.org/uc/item/0bk7n9tq>

### Author

Crandell, Philip

### Publication Date

2022

Peer reviewed|Thesis/dissertation

UNIVERSITY OF CALIFORNIA

Santa Barbara

Photomanipulation of Stress Relaxation in Alginate  
Hydrogels via Addition of PEG

A Thesis submitted in partial satisfaction of the  
requirements for the degree

Master of Science

in

Mechanical Engineering

by

Philip Crandell

Committee in charge:

Professor Ryan Stowers, Chair

Professor Jeff Moehlis

Professor Angela Pitenis

The thesis of Philip Crandell is approved.

---

Professor Jeff Moehlis

---

Professor Angela Pitenis

---

Professor Ryan Stowers, Committee Chair

June 2022

# Photomanipulation of Stress Relaxation in Alginate Hydrogels via addition of PEG

Copyright © 2022

by

Philip Crandell

## Acknowledgements

I would like to first express my thanks to my advisor, Professor Ryan Stowers for mentoring me and guiding me through my time in the Stowers Lab. I would like to express my heartfelt thanks and gratitude to him for mentoring me in good experimental techniques, experimental design, writing, presentation skills and so many other parts of being a good experimental scientist. I also very much appreciate Professor Stowers's patience while I learned many experimental techniques slowly through some trial and error during the early part of the COVID-19 pandemic. I would also like to thank Dr. Rachel Behrens at the UCSB MRL polymer facility. The polymer facility was a core part of my thesis work, and Rachel's training and insightful conversation was very helpful to me on many occasions.

I also thank Ian Tayler in the Stowers lab for his advice and tutorship over the past three years, especially for taking the time to show me specific techniques in sectioning and processing sectioned samples. I would also like to thank Professor Beth Pruitt for serving on my thesis committee and for sparking my interest in mechanobiology in general. I would also like to thank Professor Angela Pitenis for serving on my committee and for several discussions photopatterning in early stages of this project. Finally, I would like to thank all my colleagues in the Stowers lab for their feedback and support in finishing this work.

## Abstract

Hydrogel materials are commonly used to model the mechanical properties of the extracellular matrix (ECM). Viscoelastic properties of the ECM have recently emerged as a critical regulator of cellular behavior in 3D, and changes in ECM viscoelasticity are observed in fibrosis and many cancers. While hydrogel materials with tunable stiffness have been extensively used to study the effect of mechanics on cell behavior, most engineered hydrogel materials don't well recapitulate the viscoelastic properties found in the ECM. Additionally, viscoelastic properties in diseased tissue often vary in both time and space. This thesis reports a simple approach for manipulating the viscoelasticity of norbornene-functionalized alginate hydrogels via photoaddition of PEG-thiol using thiol-norbornene photoclick chemistry. Hydrogel stiffness was controlled with calcium addition, and stress relaxation controlled by addition of PEG, independently of stiffness. Addition of PEG produced gels exhibiting faster stress relaxation and increased creep. When evaluated in cells, faster relaxation led to increased cell volume and decreased sphericity in MSCs, and greater proliferation in breast cancer cells. Photopatterning of the gel embedded with MSCs led to morphologies in PEG-patterned regions consistent with fast-relaxing behavior and morphologies in non-patterned regions consistent with slow-relaxing behavior.

# Contents

Abstract .....	vi
1 Introduction .....	1
1.1 Hydrogels and viscoelasticity .....	1
1.2 Viscoelasticity in tissue biology and disease .....	5
1.3 Prior work and approach .....	8
2 Creation and testing of an alginate hydrogel with tunable viscoelastic properties .....	11
2.1 Overview of experimental work .....	11
2.2 Mechanical testing of alginates .....	14
2.3 Photoaddition of PEG to norbornene-alginate hydrogels promotes spreading in MSCs .....	17
2.4 Effects of time in slow-relaxing conditions on cell morphology .....	19
2.5 Effects of transition from slow to fast relaxing conditions on cancer cell proliferation .....	21
2.6 Spatial patterning of PEG in alginate hydrogels and effects on cell morphology.....	22
3 Discussion, conclusion, and future work .....	24
3.1 Discussion and conclusion .....	24
3.2 Future work .....	28
4 Methods .....	29
A.1 Alginate preparation.....	29
A.2 Functionalization of alginate with RGD .....	30
A.3 Functionalization of Alginate with Norbornene .....	30
A.4 Hydrogel formation and tuning of mechanical properties.....	31
A.5 Mechanical Characterization .....	32
A.6 Cell Culture.....	33
A.5 Mechanical Characterization.....	34
A.7 Morphological Staining.....	34
A.8 Proliferation Assay .....	34
A.10 Image Analysis .....	35
A.11 Statistical Analysis .....	35

B Supplemental figures .....	37
Bibliography .....	41



# Chapter 1

## Introduction

### 1.1 Hydrogels and viscoelasticity

The extracellular matrix (ECM) is a complex, structured network of structural and nonstructural macromolecules made up of the space outside cells. The ECM's composition varies widely between tissues – stiff tissues have a stiff constitutive ECM, while soft tissues have a likewise soft ECM - and complex interactions between molecules in the ECM and compositional changes in the cells that make them up continuously drive cell decision making. Changes in the mechanics of the extracellular matrix are observed in many disease and development processes, from cancer<sup>1-3</sup> to

fibrosis<sup>4,5</sup>, making study of the interaction between the ECM and cells important in understanding cell behavior and disease.

Hydrogels are the most often chosen ECM mimic for cell culture studies<sup>6</sup>, as they often have some combination of tunable stiffness, porosity or degradability, and ligand density. Early work with hydrogels focused on 2D studies, with cells grown on top of synthetic hydrogels made of polyacrylamide<sup>7</sup> or polyethylene glycol (PEG)<sup>8</sup>. Synthetic hydrogel materials with tunable stiffness have been found to elicit different mechanical responses in cells relative to hard substrates like glass and tissue culture plastic and allow for substrate stiffness resembling that found in native tissue. Small differences in elastic modulus can produce dramatically different cell behaviors including changes in adhesions<sup>9</sup>, morphology<sup>10,11</sup>, proliferation<sup>12,13</sup>, and differentiation<sup>14</sup>. While synthetic hydrogels are ubiquitous in biological contexts, other alternatives such as protein gels made from collagen, fibrin, or many different ECM proteins (Matrigel), or carbohydrate derived gels like alginate and dextran are also commonly used in tissue culture work. Mammalian protein derived hydrogels provide an advantage over other in that they naturally feature some adhesive ligands for cells, but also a disadvantage due to cost and limited tunability in terms of their chemistry<sup>15</sup>. Alginate and dextran hydrogels present no ligands to cells and have minimal natural ability to bind protein, requiring addition of peptide or proteins for cell adhesion<sup>16</sup>. All three of these classes of gels feature different crosslinking

mechanisms; PEG gels feature elastic crosslinks where covalent bonds render the gel a single large molecule<sup>17</sup>. Alginate gels are ionic in nature, meaning that a few alginate chains form “egg box”-like structures around cations<sup>18</sup>. Gels made of protein are usually formed of noncovalent interactions in vitro, with collagen being the primary example (Fig. 1A).

The extracellular matrix and other human tissues are not well modeled by elastic materials, as they also have physical properties like those of viscous liquids. While elastomers and many synthetic hydrogel materials store applied energy, many biological tissues exhibit hysteresis under cyclic mechanical loading<sup>19</sup>. Under a constant displacement or strain, many biological tissues respond with an instantaneous stress similar to an elastic material, but then dissipate stored energy in a time-dependent manner<sup>20-22</sup> (Fig. 1B). Similarly, some biological materials deform continuously under a constant applied force and have non-recoverable deformations, similar to a viscous liquid<sup>23,24</sup>. These time-dependent mechanical responses are consistent with viscoelastic material models, and are exhibited by most biological tissues. In the same way that most tissues have differing stiffness, biological tissues also vary significantly in stress relaxation. Tissues from the 100s of Pa stiffness in the brain to GPa stiffness all exhibit viscoelastic characteristics, but with differing relaxation times across a wide range of stiffnesses<sup>25</sup> (Fig 1D).

At the nanoscale, viscoelasticity is thought to arise from a mixed set of interactions (Fig. 1C). The most studied viscoelastic biomaterial, collagen I, forms helical fibrils that interact via weak forces or entanglements. The weak forces holding collagen fibrils together are transient, and can break under loading conditions, allowing for viscous responses to deformation<sup>26</sup>. After deformations, collagen matrices reform weak bonds with adjacent fibrils, leading to stored plastic deformations<sup>22,27</sup>. The mechanism of collagen deformations depends on the applied strain – under low strain rates collagen fibers break and reform bonds with adjacent fibers, but at higher strain rates collagen fibrils themselves elongate due to sliding between adjacent collagens<sup>28,29</sup>. Fibrin<sup>30</sup> and elastin<sup>31</sup> also exhibit viscoelastic properties, but due to unfolding of regions of protein that contain hydrophobic amino acid residues when exposed to stress<sup>32</sup>. Proteins that unfold under mechanical stress often aggregate due to interaction between amino acids exposed while stretched, possibly providing another mechanism for observed plastic deformations. An additional molecular source of time dependent mechanical properties is water, which causes poroelastic responses in material. Tissues are largely made up of water, and poroelastic materials lose water when deformed. Water flows into or out of the network of poroelastic materials undergoing a change in volume, resulting in an increased viscous response when tested in compression or tensions but not for materials tested in shear<sup>33,34</sup>.

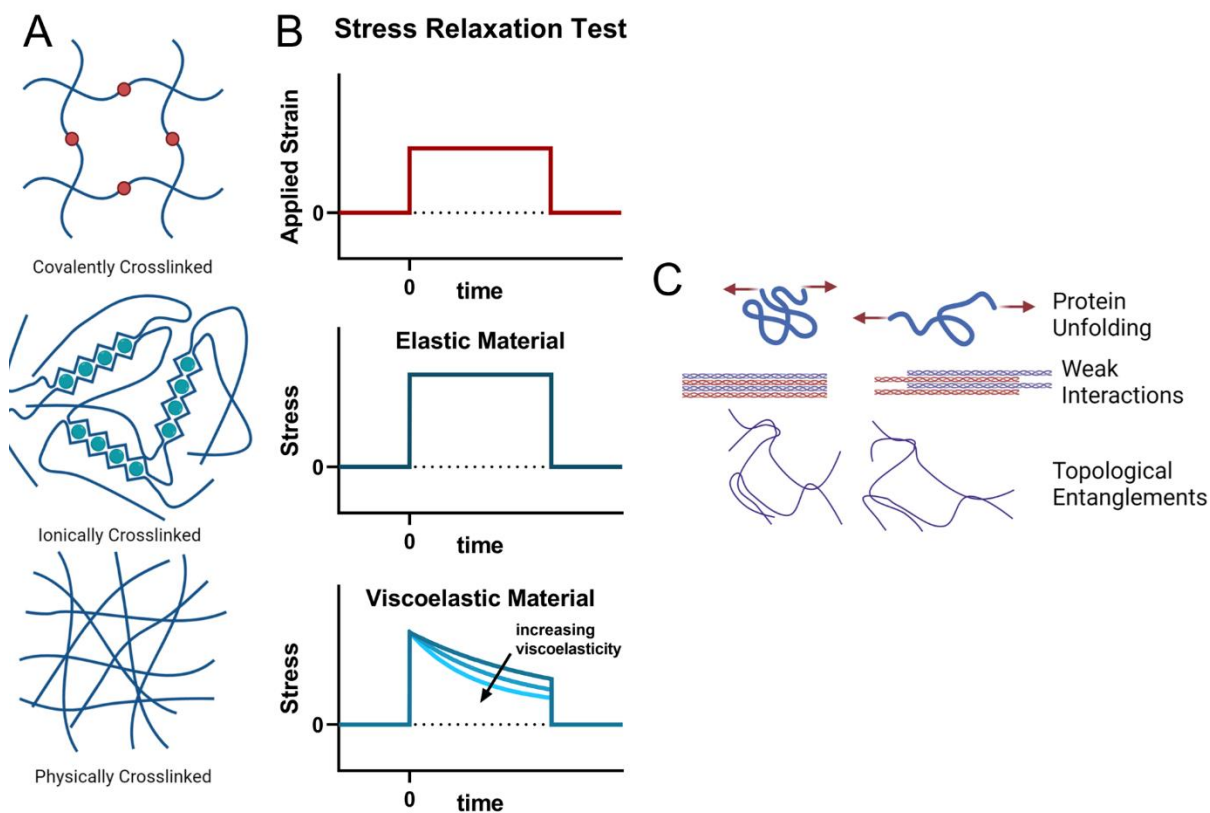


Figure 1 - Viscoelasticity in hydrogels and biological tissues A. Illustration of an idealized covalent tetra-PEG hydrogel, an ionically crosslinked alginate hydrogel and a physically crosslinked collagen gel. B. A stress relaxation test is performed using a constant strain applied quickly at time  $t=0$  (top). An elastic material (middle) will not relax, while viscoelastic materials will relax over time (bottom). C. Molecular mechanisms of stress relaxation, including protein unfolding, weak protein-protein interactions, and molecular entanglements.

## 1.2 Viscoelasticity in tissue biology and disease

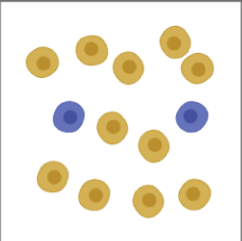
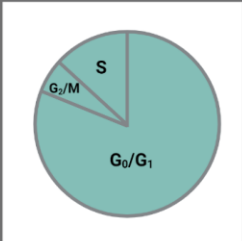
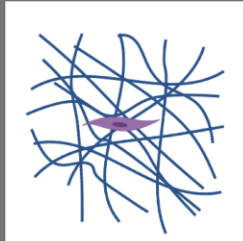
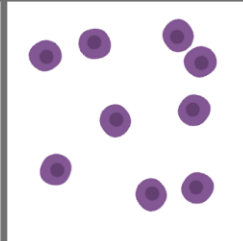
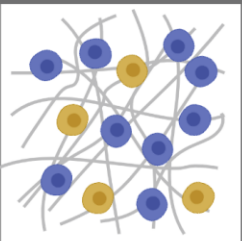
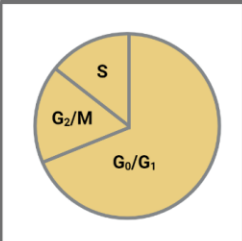
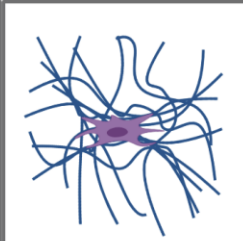
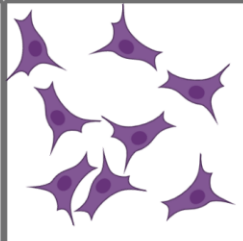
Many studies over the past two decades have demonstrated the importance of elastic modulus on cell organization, spreading, proliferation, and differentiation<sup>35-38</sup>.

Mechanistically, cells are thought to exert tractions on their substrate through their

actin cytoskeleton and activate several downstream regulatory pathways in response to substrate stiffness, ranging from integrin clustering, conformational changes in talin or vinculin, activation of mechanosensitive ion channels and multiple types of downstream transcriptional activity<sup>39,40</sup>. These interaction processes span a range of forces and timescales<sup>41,42</sup>, which can be affected by materials with time-dependent mechanical responses and can cause the interaction between cells and biological tissues to differ greatly from interactions observed between cells and more elastic hydrogels.

Several studies have explored the effects of differing degrees of matrix viscoelasticity on encapsulated cells (Fig. 2). Faster stress relaxation promotes cell spreading in fibroblasts<sup>43</sup>, MSCs<sup>44</sup>, and myoblasts<sup>45</sup>. Cells in faster relaxing networks are also known to remodel collagen fibers in an interpenetrating network or go as far as remodeling the hydrogel network itself by migrating through it or through densification via ligand clustering<sup>46</sup>. Collagen remodeling even happens across multiple scales – from local scales to tissue-wide<sup>44,47,48</sup>. Remodeling is also critical in cancer cell migration, which also occurs in networks with increased viscoelastic behavior<sup>49</sup>. Elastic hydrogels also inhibit cell cycle progression in cancer cells and fibroblasts, likely through means of mechanical confinement<sup>50</sup>. Chondrocytes and osteocytes also deposit more of their constitutive matrix in faster relaxing hydrogels relative to slower relaxing ones<sup>44,51</sup>, and MSCs are even driven towards osteogenic

fates in more viscoelastic hydrogels. Viscoelastic properties of the ECM also vary considerably in fibrosis and malignancy, both due to alterations in ECM protein makeup. Interestingly in some cases differences in viscous characteristic of tissue can be used to identify metastatic vs not metastatic tumor regions<sup>52</sup> or even separate the boundary of a tumor that has the same stiffness as surrounding healthy tissue in the case of some glioblastomas<sup>1</sup>.

Cell Differentiation	Cell Cycle Progression	ECM Remodeling	Cell Spreading	
				<b>Slow Relaxing</b>
				<b>Fast Relaxing</b>

**Figure 2 - Role of viscoelasticity on cell fate and in disease** Chart showing illustrated effect of fast versus slow relaxing substrates on individual cells. Fast relaxing conditions promote more spread and stellate morphology in fibroblasts, remodeling of collagen fibrils in Type I collagen gels, more time in replicative portions of the cell cycle, and matrix deposition and cell differentiation.

### 1.3 Prior work and approach

Hydrogels with tunable stress relaxation take on a variety of forms. Tunable viscoelasticity can be accomplished using dynamic or transient crosslinks<sup>45,53,54</sup>, modifying the polymer density and crosslink density together<sup>45,55,56</sup>, or by adding crosslinking modalities that have interactions weaker than covalent or even ionic interactions<sup>57-59</sup>. Alginate (Fig. 3A) is a naturally derived hydrogel that is ionically crosslinked and is often used as a viscoelastic substrate. Alginates of lower mass need a higher crosslinking (ionic) density to form a stable network but make up a more viscoelastic network than higher mass alginates crosslinked with fewer ions, due to their higher chain mobility<sup>43</sup>. Alternatively, prior work has shown that grafting monofunctional PEGs of onto higher molecular weight alginate also increased the viscoelastic behavior of higher molecular weight alginate hydrogels with PEGs possibly reducing entanglement interactions between alginate chains<sup>44,60</sup> (Fig 3B). Grafting of 5kDa PEG was found to vary the stress relaxation behavior of higher molecular weight alginate across nearly two orders of magnitude (Fig 3).

However, most existent systems for modifying the stress relaxation of hydrogel materials do not allow for stress relaxation properties to be modified independently of stiffness in situ, instead often requiring dissolution of the gel and encapsulation, a process that is typically stressful and often deadly to cells. Because viscoelasticity often varies in time and space in disease models, we felt it important



to try to develop a system that recapitulates these characteristics via photochemistry. A few groups have developed system with phototunable stress relaxation, although all had the weaknesses of limited tunability, limited independence between stress relaxation and stiffness, or only transitioning towards less viscoelastic behavior<sup>61-63</sup> (Table 1). With these characteristics in mind, we sought to develop a phototunable alginate system that allows for a similar range of tunability as achieved in prior work but performed in-situ and in mild conditions.

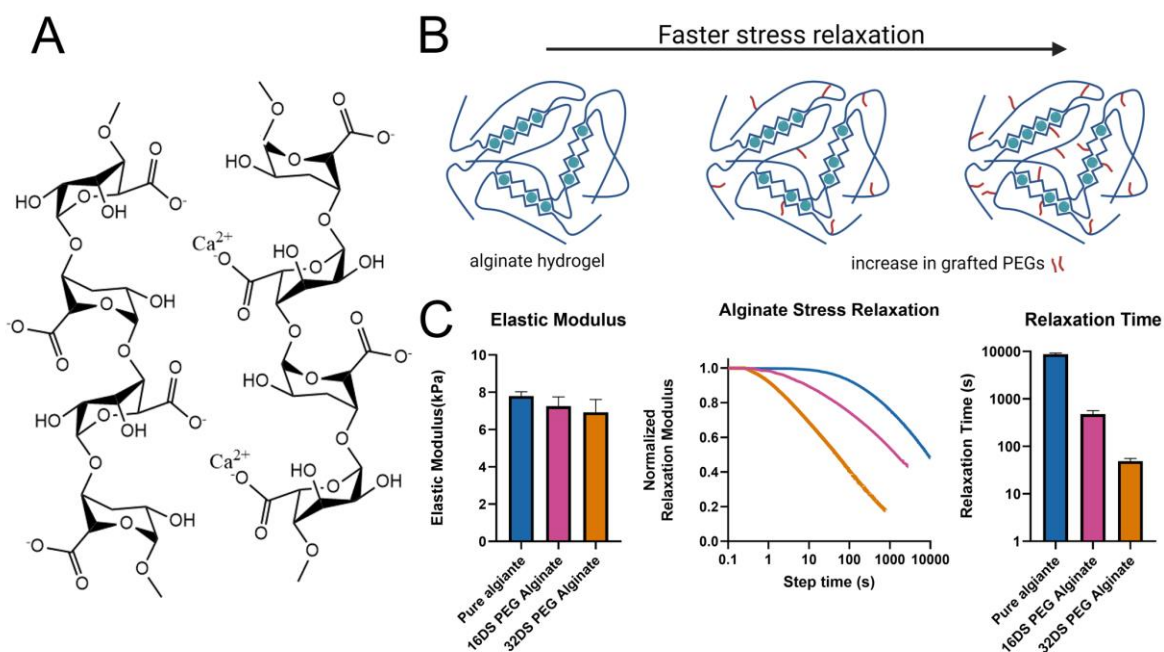


Figure 3 - Prior work on tunable viscoelastic alginate materials A. Structure of alginate, showing the interaction between carboxylic acid groups and divalent calcium ions. B. A cartoon of PEG of increasing masses being covalently added to alginate C. Data showing the stress relaxation effects of adding PEG to HMW alginate in differing degrees of substitution.

Gel substrate	Crosslink Mechanism	Viscous mechanism	Viscoelastic change	Author
PEG	Thiol-norbornene links	Thioester exchange	Becomes less viscoelastic	62
PEG	Dynamic covalent links	Dynamic covalent exchange	Either	61
Hyaluronic acid	Thiol-norbornene links	Host-guest interactions	Becomes less viscoelastic	60

Table 1 - Prior work on phototunable viscoelastic hydrogel materials, and their characteristics

## Chapter 2

# Creation and testing of an alginate hydrogel with tunable viscoelastic properties

### 2.1 Overview of experimental work

First, we modified alginate polymers known to have slow stress relaxation with norbornene functional groups to facilitate grafting of monofunctional PEGs. Alginate hydrogels are a common 3D cell culture substrate known to exhibit stress relaxation when ionically crosslinked. Norbornene methylamine was grafted to alginate using carbodiimide chemistry, a well-established chemistry<sup>64</sup> for

functionalizing amines to alginate's carboxylic acid groups (Fig. 4A). Quantification of this reaction using Ellman's reagent found that 7% of the carboxylic acids used in this experiment were substituted with free thiols (Fig. 12). Norbornene functional groups can react with free thiols in solution in the presence of a photo-initiator via the cytocompatible thiol-ene reaction (Fig. 4A). Which has been shown to produce changes in stress relaxation depending on the amount of PEG added<sup>60,65</sup> (Fig. 4B). This, in turn produces downstream changes in cell proliferative behavior and morphology (Fig. 4C)

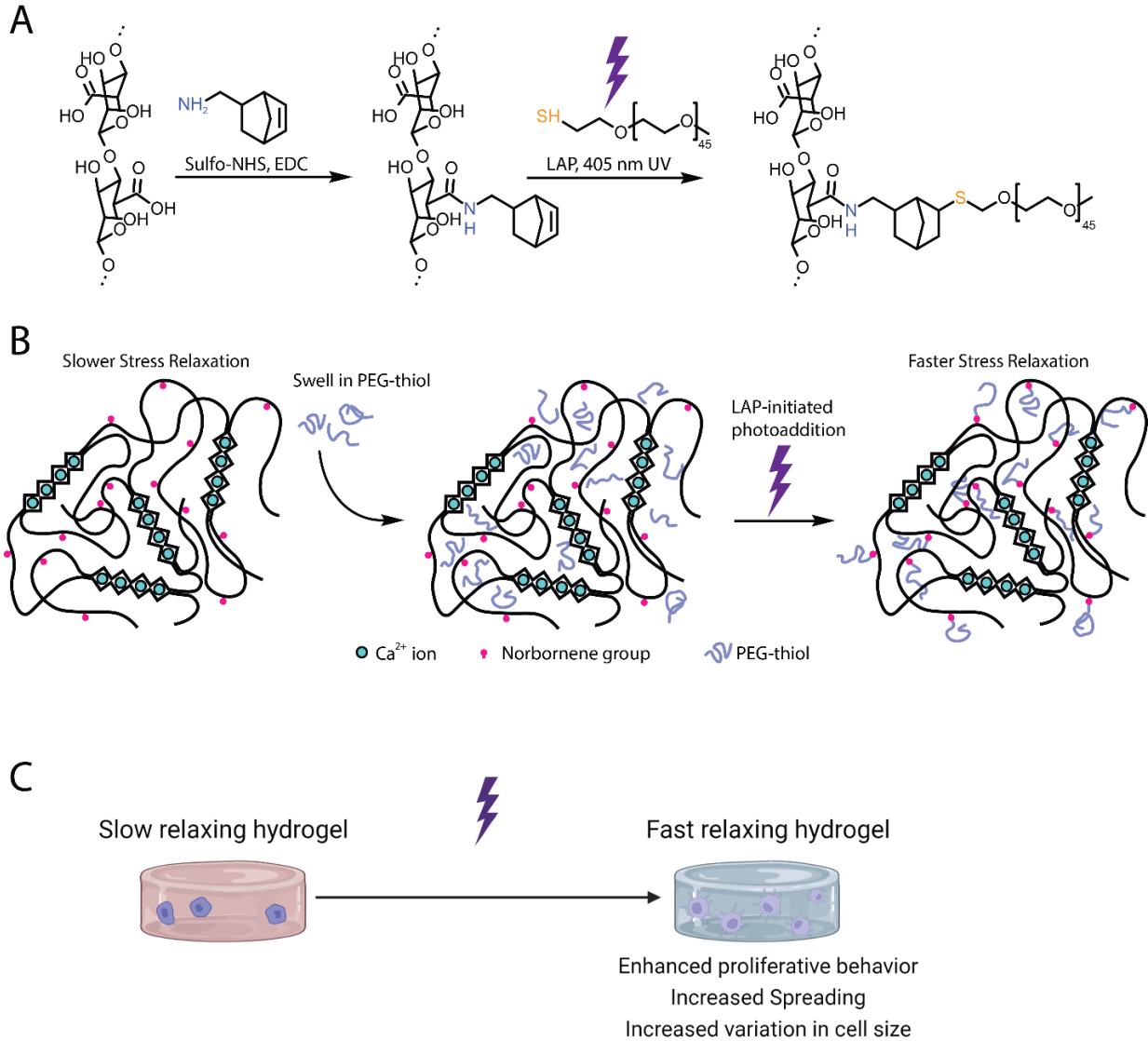


Figure 4 - Photoaddition of PEG to tune stress relaxation in Alginate hydrogels functionalized with norbornene. A. Diagram shows the chemical steps involved in attaching PEG to alginate. Amine terminated norbornene is functionalized to alginate using NHS-EDC coupling. Norbornene-alginate reacts with PEG-thiol in the presence of photoinitiator and UV light. B. Molecular cartoon drawing shows Norbornene functionalized alginate crosslinked with calcium before and after introduction of PEG. C. Changes in stress relaxation produce morphological changes and increases in proliferation in cells.

## 2.2 Mechanical testing of alginates

Conjugation of PEG to alginate has been shown to produce changes in stress relaxation. Here, we sought to measure the effects of PEG photoaddition to alginate hydrogels. To approximate PEG-addition in cell-culture conditions, norbornene-alginate hydrogels were ionically crosslinked, cut into 8mm circular samples with a biopsy punch to ensure samples had the same initial mechanical properties. To modify mechanical properties after gelation, samples were placed in buffers containing monofunctional 2 kDa PEG-thiols, exposed to a violet laser source, then allowed to swell in buffer to remove any unreacted material (Fig. 5A). Alginate hydrogels with a larger ratio of PEG-thiols to norbornene produced faster relaxing hydrogels (Fig. 5B, 13). Quantification of stress relaxation was taken by calculating the relaxation time ( $\tau_{1/2}$ ) for each group (Fig. 5C, 14), and amplitude sweeps were performed to verify stress relaxation occurred in the linear viscoelastic region (Fig. 11). Relaxation times varied from 840 seconds for unmodified alginate to 82 seconds for hydrogels where the concentration of added thiol exceeded the number for norbornene groups. Adding PEG in a 1.6 molar excess to norbornene produced similar stress relaxation times to a 1.2 molar excess, indicating that there is a diminishing effect at high PEG concentrations. Despite the enhanced stress relaxation rate with PEG photoaddition, the elastic moduli were similar to unmodified alginate gels for both relatively soft and stiff hydrogels (Fig. 5D, 15).

Additionally, creep-recovery testing was then performed on unsubstituted and 1.2:1 thiol: norbornene hydrogels. In a creep-recovery test a constant stress is applied to the gel for a certain time, followed by a longer period of zero stress allowing the gel strain to recover. PEG-substituted hydrogels had significantly higher residual strains after creep-recovery testing, indicating more plastic deformation in these gels, (Fig. 5E). Frequency sweep data of alginate hydrogels showed significantly increased lossy behavior on longer timescales (Fig. 12). Together these results show that photoaddition of PEGs in alginate hydrogels can allow for on-demand changes in stress relaxation and creep behavior of alginate hydrogels independent of elastic modulus.

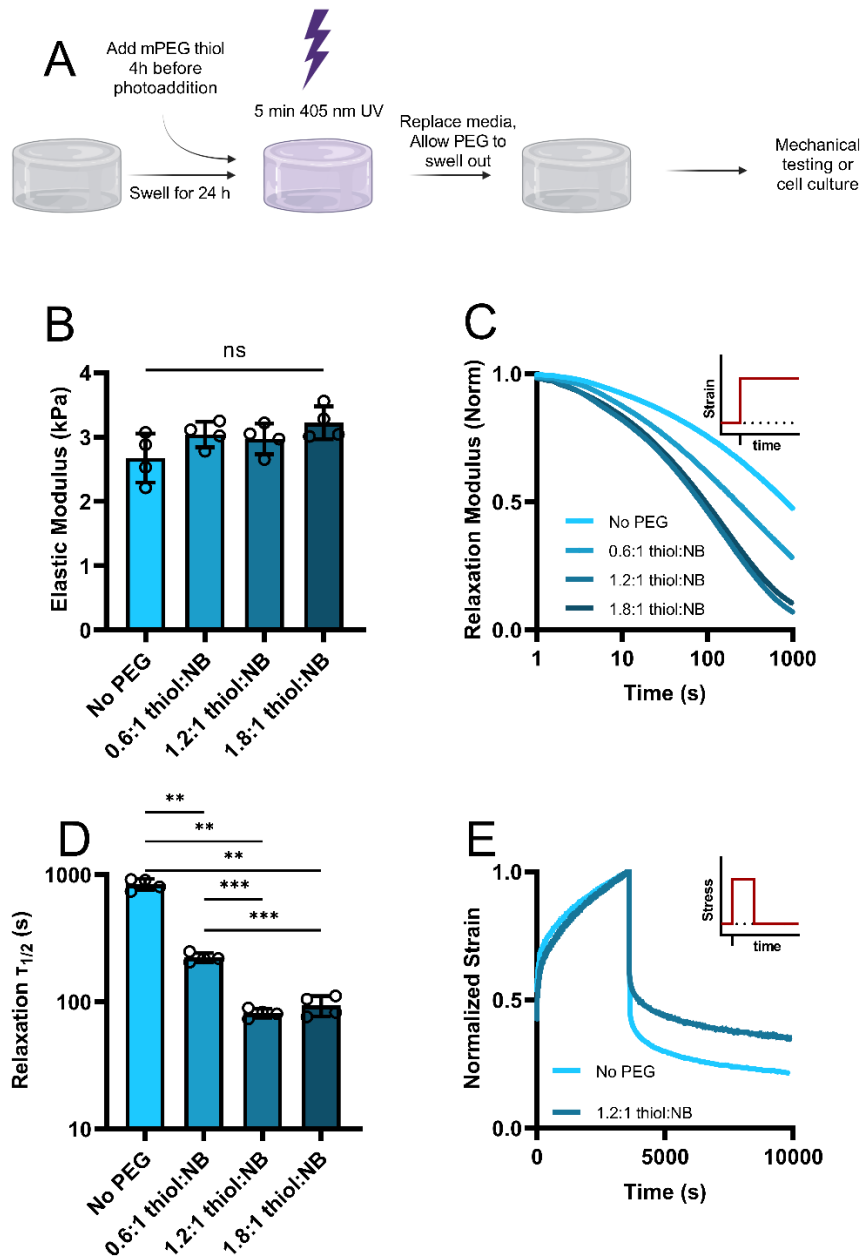


Figure 5 - Alginate - norbornene hydrogels can be modified to exhibit faster stress relaxation when grafted with PEG thiols. A. Experimental overview of photoaddition of PEG-thiols to alginate-norbornene. B. Stiffness of alginate hydrogels with differing amounts of photo-grafted PEG. C. Stress relaxation tests of alginate-norbornene gels in B with different ratios of added PEG. D. Quantification of Relaxation times in C, showing the time taken for stress to reach half its initial value. E. Creep-relaxation testing of the No PEG and fully substituted PEG-alginate hydrogels. Statistics in B and D were performed using a Kruskal-Wallis multiple comparisons test, with \*\*, \*\*\*, and \*\*\*\* indicating  $p < 0.01$ ,  $p < 0.001$ , and  $p < 0.0001$ , respectively



## 2.3 Photoaddition of PEG to norbornene-alginate hydrogels

### promotes spreading in MSCs

After establishing that our norbornene-alginate hydrogels have phototunable viscoelastic properties, we then sought to determine how cells respond to dynamic changes in stress relaxation rates. Alginate does not possess binding sites for cell adhesion, so peptides presenting the RGD-binding motif were coupled to norbornene-alginate to allow for cell adhesion, as described previously<sup>44</sup>. Prior reports have demonstrated that mesenchymal stem cells (MSCs) have increasing protrusions and spreading in fast relaxing matrices compared to rounded morphologies in slow relaxing matrices<sup>44</sup>. We sought to determine if cell spreading could be induced on-demand by triggered a transition from slow relaxing to fast relaxing conditions in the presence of cells. (Fig. 6A). The amount of time in slow-relaxing conditions before PEG addition was varied for encapsulated mouse D1 MSCs. As expected, cells cultured in slow relaxing matrices for 7 days were very rounded with few protrusions (Fig. 6B). Intriguingly, cells in matrices that were transitioned from slow relaxing to fast relaxing were significantly less round, displayed numerous protrusions, and had significantly larger volumes (Fig. 6B-E). This effect depended on the time of transition, with a diminished effect for cells cultured in slow relaxing matrices for extended time periods initially.

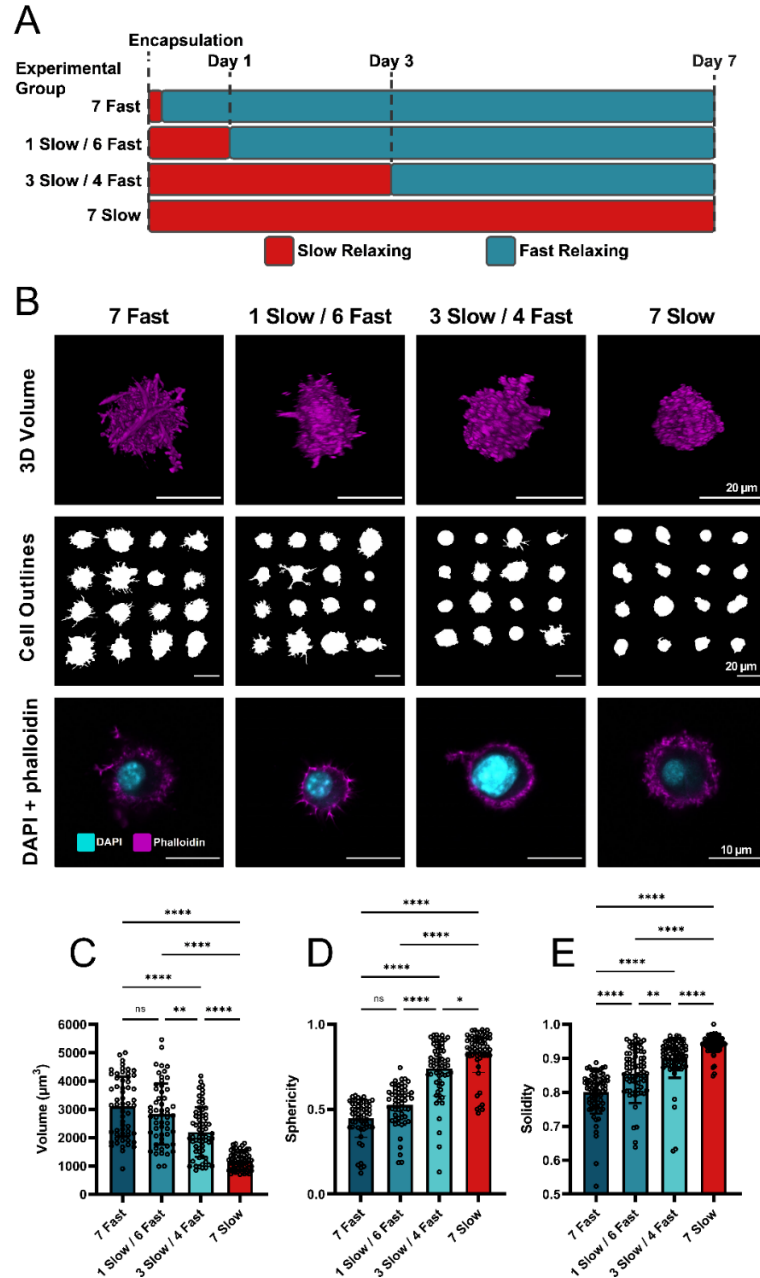


Figure 6 - Photoaddition of PEG to norbornene-alginate hydrogels promotes cell spreading

A. Timeline for each experimental group in panels B-E, showing time spent in fast and slow relaxing conditions. B. Representative 3D renderings (top row), outlines (middle row), and representative morphologies (bottom row) of mouse D1 cells at the end of 7 days in each condition. In the bottom row phalloidin fluorescence is shown in pink and DAPI in cyan. C. Volume of cells in each condition D. Sphericity of cells in each condition and E. 2D solidity of cells in each condition.

## 2.4 Effects of time in slow-relaxing conditions on cell morphology

To distinguish the influence of the initial culture period in slow relaxing matrices from the total time in fast relaxing matrices (both of which were varied in the experiments in Figure 3), we varied the time in the initial slow relaxing matrices but maintained the cells in the fast-relaxing matrices for 7 days for all groups. (Fig. 7A). Morphological differences relating to time in slow relaxing conditions are less visually pronounced between all groups in fast-relaxing conditions (Fig. 7B). Cell volumes are similar between all groups in fast conditions between 0 and 3 days (Fig. 7C), but higher than fast relaxing conditions, and sphericity and solidity (Fig. 7 D-E) are significantly lower in each group that spent 7 days in fast relaxing conditions. Together, this indicates that MSCs seem exhibit different morphologies in slow and fast relaxing conditions, with time spend in slow relaxing conditions having little to no effect on cells after transitioning to faster conditions.

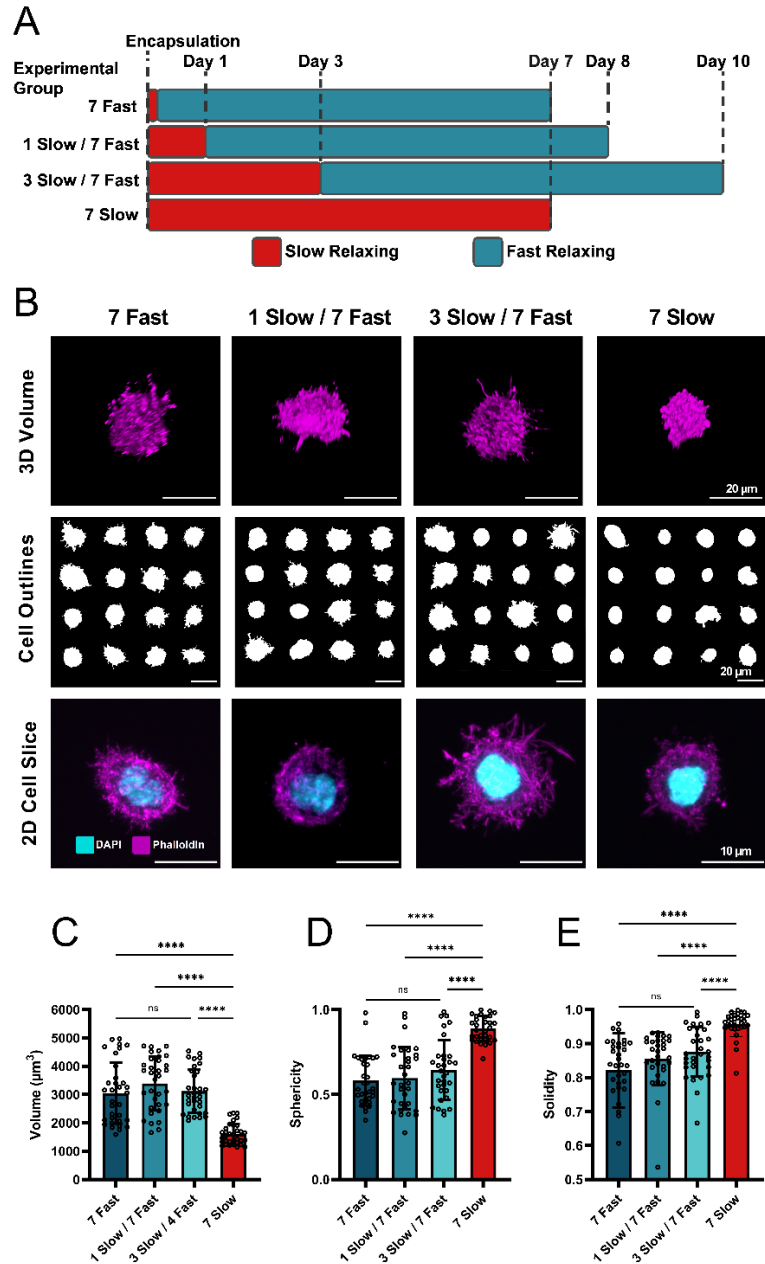


Figure 7 - Cell spreading in PEG-Alginate hydrogels does not depend on time spent in slow-relaxing conditions

A. Timeline for each experimental group in panels B-E, showing time spent in fast and slow relaxing conditions. B. Representative 3D renderings (top row), outlines (middle row), and representative morphologies (bottom row) of mouse D1 cells at the end of 7 days in each condition. In the bottom row phalloidin fluorescence is shown in pink and DAPI in cyan. C. Volume of cells in each condition D. Sphericity of cells in each condition and E. 2D solidity of cells in each condition.

## 2.5 Effects of transition from slow to fast relaxing conditions on cancer cell proliferation

In addition to assessing the cell morphology in gel with varying stress relaxation, we also assessed proliferation of cells in slow and fast conditions. Stress-relaxation conditions were adjusted from slow to fast-relaxing after 0, 1 or 3 days in culture, and all samples were fixed after 5 days (Fig. 8A). Cell-cycle progression was monitored by incorporating EdU after 4 days of culture (Fig. 8B). In each condition a significantly higher number of cells stained EdU positive after 5 days while in fast relaxing conditions as compared to cells in slow relaxing conditions as compared to slow relaxing conditions (Fig. 8C).

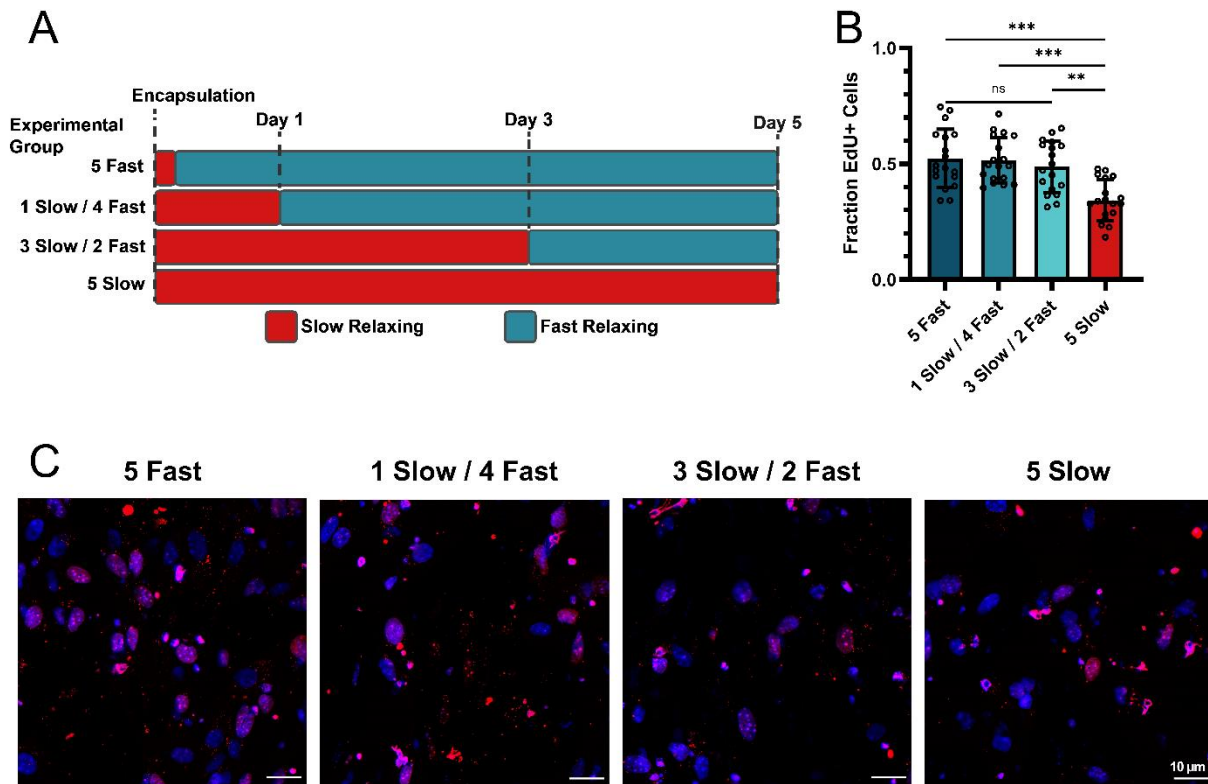


Figure 8 - PEG photoaddition promotes cell cycle progression in alginate hydrogels.

A. Timeline of PEG photoaddition experiment with MDA-MB-231 cells. B. Fraction of EdU positive cells in each cultured condition. C. Microscopy images of cells in each PEG photoaddition condition. One-way ANOVA and Dunn's comparison tests were used in B, \*\* indicates  $p < 0.01$  and \*\*\*  $p < 0.001$ .

## 2.6 Spatial patterning of PEG in alginate hydrogels and effects on cell morphology

While photoaddition allows easy modification of alginate stress relaxation properties over time, thiol-norbornene reactions can straightforwardly be photopatterned, potentially allowing spatial control of cellular behavior. To this end, we patterned hydrogels using a collimated laser source and a simple laser-printed

photomask. To view the resulting patterns, 5% of the PEG used was labeled with FITC, enabling viewing of the pattern via a fluorescent microscope. Simple patterns could be easily made in a chambered cover glass or glass bottom plate, with decent fidelity (Fig. 9A). To attempt to quantify the pattern fidelity in 3D with this system, we patterned gel with lines of decreasing widths. Although pattern fidelity is good near the bottom of the gel (Fig. 9B), lines thinner than 50  $\mu\text{m}$  are not preserved through the gel structure (Fig. 6C). Using these limitations, we patterned a gel containing D1 MSCs with fluorescent PEGs with 250  $\mu\text{m}$  lines and fixed the gel after 7 days. Using a tiled scan of the whole gel, differing morphologies can be observed in regions with and without PEG (Fig. 9D). Cell morphologies in regions with and without PEG differed in quantified area, circularity, and solidity (Fig. 9E-G). Cells in PEG patterned regions showed greater areas and decreased circularity and solidity, indicative of their greater number and size of protrusions. Overall, we demonstrate that this system can be used to pattern gels spatially, and that cells elicit a similar morphological response to being in a fast-relaxing local region of a gel as they do to being in an entirely fast-relaxing gel.

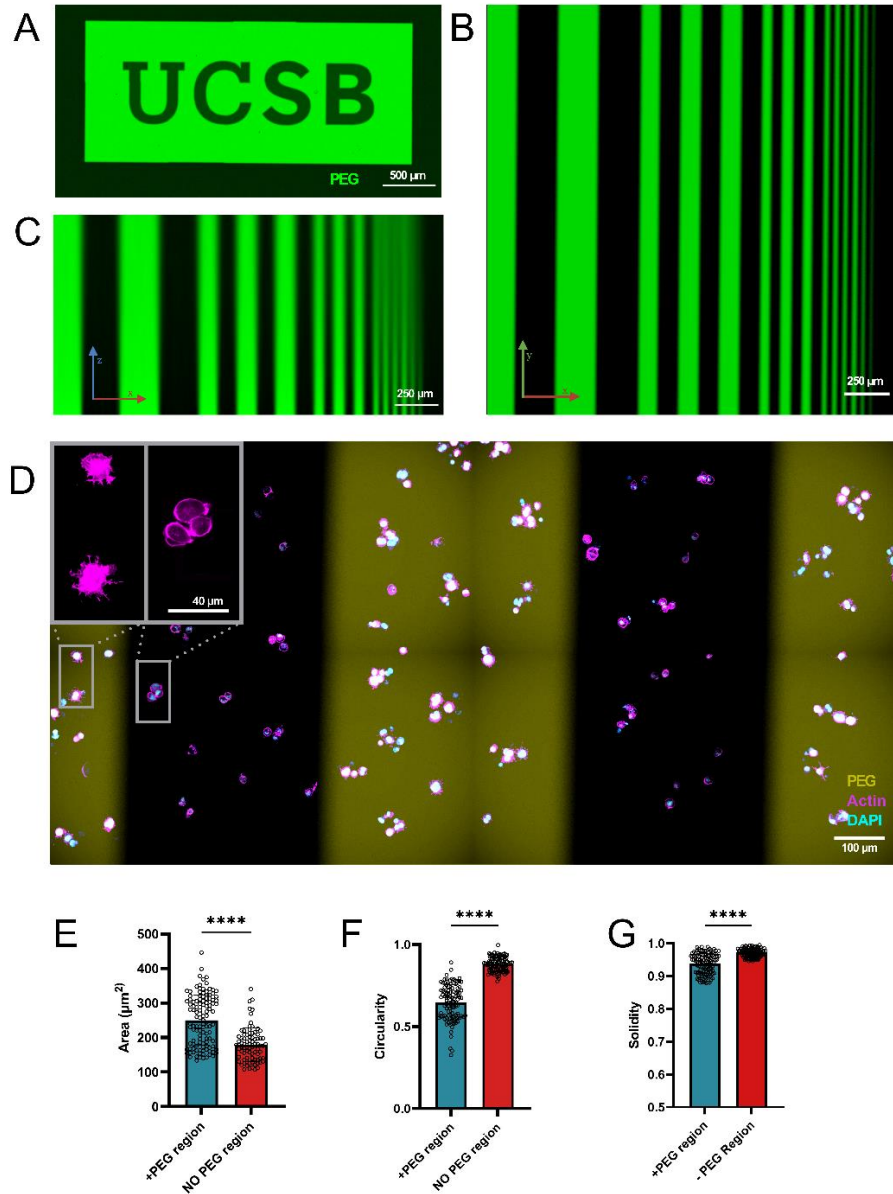


Figure 9 - Spatially patterned PEG allows for control of cell phenotype within the same gel.

A. 2D FITC-PEG-thiol patterning example, scale bar is 500  $\mu\text{m}$ . B. Bottom-up image of a patterned hydrogel, showing reproduction of the original pattern, alginate with C. A maximum intensity projection of a x-z slice of the gel. Scale bars in B and C are 250  $\mu\text{m}$ . D. Shows cells seeded in a gel patterned with 250  $\mu\text{m}$  stripes – FITC-PEG stripes are rendered in yellow, phalloidin an magenta and DAPI in cyan. Scale bar is 100  $\mu\text{m}$ . E. Roundness of cells from regions with and without photopatterned PEG, F and G show circularity and solidity from those regions, respectively. \*\*\*\* indicates  $p > 0.0001$  using the Kolmogorov-Smirnov comparison test.



## Chapter 3

### Discussion, conclusion, and future work

#### 3.1 Discussion and conclusion

In summary, this thesis demonstrates a straightforward method to produce alginate-based cell culture substrates with viscous properties that can be tuned after gel formation via photopatterning of PEG. The alginate hydrogel's viscous properties vary independently of the elastic moduli and can be adjusted by modifying either the concentration of calcium or the concentration of alginate. Photoaddition of a commercially available PEG-thiol allows for straightforward modification of alginate viscoelasticity. Previous work has shown changes in stress relaxation of alginates

when grafted covalently with PEG before gelation, but here we show the effects of PEGs added to ionically crosslinked alginate gels. We also show that stress relaxation becomes faster proportional to the concentration of added PEGs up to the saturation limit of the norbornene functionalized to the alginate hydrogels. PEG-modified norbornene-alginate hydrogels also showed increased creep during creep relaxation testing, again indicating that photoaddition of PEG increases the viscoelastic character of the alginate hydrogels.

We also tested these PEG modified alginate hydrogels for their use as a 3D cell culture platform. Of particular interest was the ability to add PEG some time after gelation, to allow cells to spend time in a slow relaxing condition, and then spend time in a fast-relaxing condition, a change that has relevance to previous studies that have observed cells having mechanical memory of previous stiffness conditions and to relevance certain types of cancer<sup>42</sup>. Previous studies have found that fast relaxing hydrogels promote cell spreading and cell cycle progression while slower relaxing hydrogels do not. Fast relaxing hydrogels in this study were also found to facilitate MSC spreading, with cellular spreading and volume proportional to the total number of days these cells spent in fast-relaxing conditions. MSCs were also not observed to have any significant memory of time spent in slow relaxing conditions, as cells displayed similar phenotypes after 7 days in fast relaxing conditions, despite spending up to 3 days in slow relaxing conditions before the

transition. Transition to fast relaxing conditions also enhanced cell proliferation as reported by others. Thiol-norbornene photoaddition is also well suited to photopatterning, and photopatterned fluorescent PEGs were used to produce striped patterns into the volume of the gel with fidelity of the same order of magnitude as the cells contained in the gel. MSCs in a photopatterned gel again exhibited morphologies consistent with being placed in fast or slow relaxing conditions.

### 3.2 Future Work

The work presented in this thesis introduces a new method to tune the stress relaxation of alginate hydrogels, allowing gels to transition from fast relaxing to slow relaxing with both temporal and spatial control. While these are useful conditions, the ability to transition from slow to fast relaxing is more physiologically relevant to other disease states, such as cancer, wound repair, and fibrosis<sup>25</sup> than a transition from slow to fast relaxing conditions. Photocleavable hydrogels are the subject of considerable research, and removal of PEG via photocleavage or exchange would likely be another way to facilitate transitions of stress relaxation in both directions. Another possible approach would be to facilitate the addition of bifunctional PEGs with an end group with tunable properties allowing for hydrophobicity or adhesion to be turned off or on, which might interfere with PEG's inherent effects on alginate viscoelasticity.

Another direction of interest would be using the photoaddition capabilities of this system to work with addition of new peptide or protein ligands or adhesion molecules, potentially allowing simultaneous exploration of the effects of ligand type and mechanical conditions within the same gel, and area of considerable research interest

# Appendix A

## Methods

### A.1 Alginate preparation

Alginate (280 kDa molecular weight, LF20/40) from FMC biopolymer was dissolved at 1% in deionized water and dialyzed with 10 kDa MWCO membranes against deionized water for 3 days. Following dialysis, alginate was purified with activated charcoal, sterile filtered, frozen, and lyophilized.

## A.2 Functionalization of alginate with RGD

RGD peptides were coupled to alginate using carbodiimide chemistry. Alginate was dissolved in MES buffer, with pH adjusted to 6.5. Then, appropriate amounts of sulfo-NHS (N-hydroxysulphosuccinimide, TCI Chemicals), N-(3-dimethylaminopropyl)-N'-ethyl carbodiimide hydrochloride (EDC, Sigma-Aldrich), and GGGGRGDSP (Peptide 2.0) and the reaction was left to stir for 20 h at room temperature. The product was then transferred to 10 kDa MWCO dialysis tubing and dialyzed against decreasing concentration NaCl solutions starting from 120 mM to 0 mM over 2 days followed by 1 day of dialysis against deionized water. Water was then removed via lyophilization to yield functionalized alginate (Alg-RGD)

## A.3 Functionalization of Alginate with Norbornene

Alginate functionalized with RGD was additionally functionalized with norbornene using a similar procedure to the above. Alginate-RGD was dissolved in MES buffer and functionalized with sulfo-NHS, EDC, and norbornene (5-norbornene-2-methylamine, TCI Chemicals). After allowing sulfo-NHS, EDC and alginate-RGD to dissolve, the pH of the MES was raised to 8, and norbornene was added. Following the reaction, the alginate was dialyzed and lyophilized as described above.

Lyophilized alginate was dissolved in phenol red-free DMEM at 3% M/V. Free

norbornenes were quantified by reacting with 2kDa mPEG-thiols (Laysan Bio) and Ellman's reagent ((5,5-dithio-bis-(2-nitrobenzoic acid), Sigma) Remaining thiols were quantified with Ellman's reagent to determine norbornene substitution of alginate.

#### A.4 Hydrogel formation and tuning of mechanical properties

To tune the viscoelasticity of alginate after gelation, mPEG-SH chains were reacted with norbornene groups on alginate. Alginate gels were formed, as described previously<sup>66</sup>. Briefly, a syringe containing alginate was coupled to a second syringe containing calcium sulfate in DMEM and the contents of both syringes were rapidly mixed. Hydrogels were cast directly into 8-well chambered cover glasses or cast between two silanized glass plates spaced 2mm apart and punched into 8mm discs. After gelation for 40 minutes at 37 C, gels were equilibrated in DMEM. To photocouple PEG, PEG-thiol and LAP (Lithium phenyl-2,4,6-trimethylbenzoylphosphinate, Sigma-) in phenol red-free DMEM were added to the well either after immediately post-gelation, or after 24 or 72 hours. PEG was allowed to swell in for 4 hours, then gels were exposed to 60 seconds of 405 nm light, and the media was changed to remove any unreacted PEG.

## A.5 Mechanical Characterization

Hydrogel mechanical properties were characterized on a TA Instruments ARES G2 strain-controlled rheometer with 8 mm parallel plates. Alginate hydrogels with and without PEG were formed as described above. All hydrogel samples were measured 24 hours after photoaddition of PEG, if applicable. The top plate was brought down until it registered a non-negative axial force, and the gap between plates was filled with DMEM. Shear modulus was measured using a frequency sweep from 0.1 to 10 Hz at a strain of 0.01. Elastic modulus was calculated from measured shear and loss moduli, assuming a Poisson's ratio of 0.5 and  $E = 2G^*(1+\nu)$ , where  $G^*$  is the complex modulus, calculated as  $G^* = \sqrt{G'^2 + G''^2}$ .  $E$  is the elastic modulus,  $G'$  is the storage modulus,  $G''$  is the complex modulus, and  $\nu$  is Poisson's ratio. For stress-relaxation tests, a strain of 15% was applied, and stress was recorded over time. Relaxation time was defined as the time taken for the stress to relax to half of its initial value. For creep tests, a constant 100 Pa stress was applied to each alginate gel for 3600s and the gel was allowed to recover at 0 Pa applied stress for 7200s. Control values for each creep-recovery test were derived via a frequency sweep performed directly before the test.



## A.6 Cell Culture

Mouse D1 MSCs (ATCC, CRL-12424) were cultured in Dulbecco's Modified Eagles Medium (DMEM, Gibco) with 10% fetal bovine serum (Gibco) and 1% penicillin/streptomycin (Invitrogen). Mouse D1 cells were passaged at approximately 50% confluency and the media was changed every 48 hours. MDA-MB-231 cells (ATCC, HTB-26) were expanded in DMEM containing 10% fetal bovine serum and 1% penicillin/streptomycin (Gibco). The medium was changed every 48 hours and the cells were passaged at 70 % confluency.

## A.7 Morphological Staining

For cell morphology staining, cells were grown in hydrogels cast into a chambered cover glass (Nunc Lab-Tek II, Fisher). After the last day of the culture period, cells were fixed using 4% paraformaldehyde in serum-free DMEM at 37C for 1 hour. Gels were then washed 3 times in PBS containing calcium and 0.1% Triton X-100 for 30 minutes each. Alexa Fluor 555 phalloidin and DAPI were added for 90 minutes at room temperature, and the sample was again washed 3 times with calcium PBS at

30-minute intervals. Samples were imaged immediately using a Leica SP8 with a 25x water immersion objective.

## A.8 Proliferation Assay

To quantify proliferation, cells were encapsulated in hydrogels as described above and media containing 10  $\mu$ M EdU (5-Ethynyl-2'-deoxyuridine, Click Chemistry Tools) was added 24 hours before fixation. After fixation, gels were fixed in 4% paraformaldehyde for 45 minutes, washed 3 times with PBS containing calcium (Gibco), and incubated with 30% sucrose (Fisher) in calcium-containing PBS overnight. Gels were then placed in a mixture of 50% sucrose and 50% OCT (Tissue-Tek) on a shaker for 8 hours before being frozen on oct and sectioned. Sectioned gels were stained for EdU using a 647 fluorescent EdU kit (Click-&-Go EdU 647, Click Chemistry tools) per the manufacturer's directions. After functionalizing EdU with Fluorophore, sections were incubated in 1:1000 DAPI for 30 minutes and washed 3x with PBS.

## A.9 Photopatterning of Alginate

Patterned photomasks were produced using a laser printer to transfer toner to an 8x10 Shrinky-Dink sheet. Sheets were then cut and placed in an oven at 160 °C for

two minutes, similarly, to previously described methods<sup>67</sup>. A glass slide was placed on the Shrinky-dink as it shrunk to ensure the pattern stayed flat during shrinking. Patterns were formed in samples in a chambered-bottom coverglass using a collimated 405 nm laser (NDV4512, Laserlands) and by placing the pattern against the glass surface of the sample and illuminating through it for 30 seconds.

### A.10 Image Analysis

All images were collected using a Leica SP8 confocal microscope using a 0.95 NA 25x water immersion objective. Metrics describing cell morphology in three dimensions such as sphericity and volume were quantified using Bitplane Imaris 9.5 software. In Imaris, sphericity is defined as the ratio of the surface area of a sphere with the same volume as the cell to the surface area of the cell itself. Solidity of a maximum projection of a 3D stack was quantified using ImageJ, where solidity represented the difference between the convex hull area and the area of the cell itself. All 2D images of cell proliferation staining were analyzed and quantified by counting the number of co-stained DAPI and EdU cells and taking that as a fraction out of each separate field of view. Morphology experiments were analyzed using images patterned gels were performed from a single stitched stack from 3 technical replicates, each 50  $\mu\text{m}$  deep and 3 square mm area.

### A.11 Statistical Analysis

Statistical comparisons were performed using GraphPad Prism 9.5. One-way analysis of variance was used to compare more than two groups. For measurements like cell volume, sphericity, and solidity the D'Agostino-Pearson normality test was first performed to test if the data could be treated normally. For cell morphology experiments approximately 25 cells were collected per trial and data from 3 separate trials was pooled for analysis. A total of 18 fields of view were analyzed from 2 separate trials in each condition. Morphology experiments were analyzed. Image analysis of patterned gels was performed from a single stitched stack from 3 technical replicates. Cells from photopatterned gels were analyzed using 2D metrics because the vertical sampling rate was insufficient for 3D analysis, and values for circularity, roundness, and solidity were reported.

# Appendix B

## Supplementary Figures

B.1

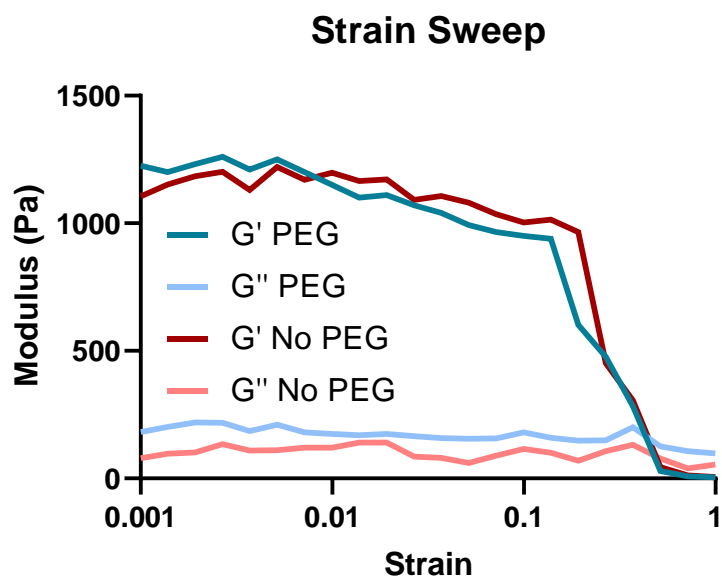


Figure 10 - Strain sweep of PEG modified and unmodified hydrogels. PEG modified hydrogels were tested in shear at strains from 0.1% to 100%.

B.2

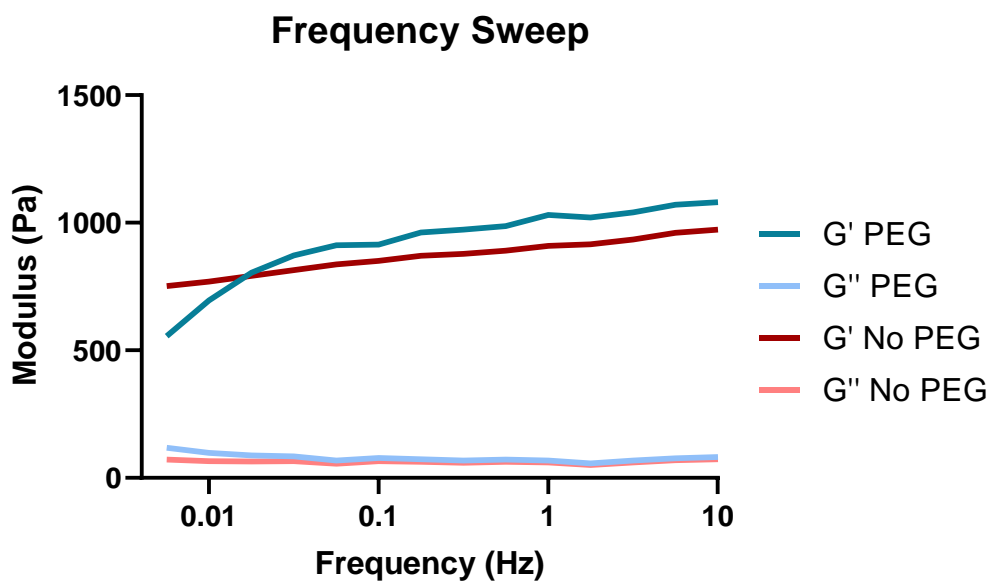


Figure 11 - Frequency sweep of PEG modified and unmodified hydrogels. Gels were tested from 10 Hz to 0.0075 Hz.

B.3

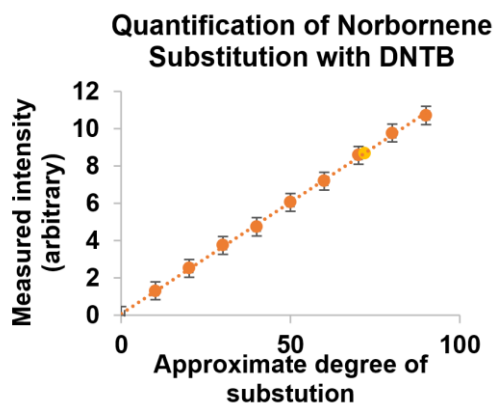


Figure 12 - Quantification of Norbornene Substitution using Ellman's Reagent (DNTB). Ellman's reagent was used to detect unreacted PEG thiols against a standard curve of soluble norbornene.

B.5

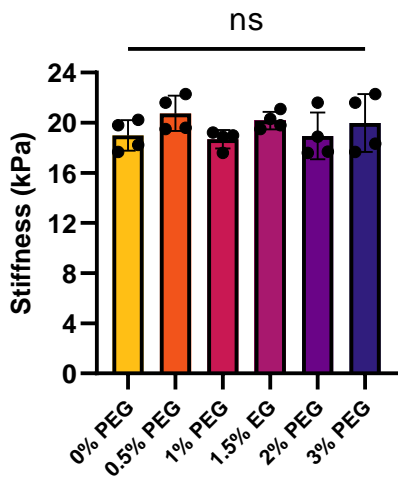


Figure 13 - Elastic modulus of 2% norbornene-alginate with added PEG. N=4 for each group, compared using the Kruskal–Wallis test.

B.6

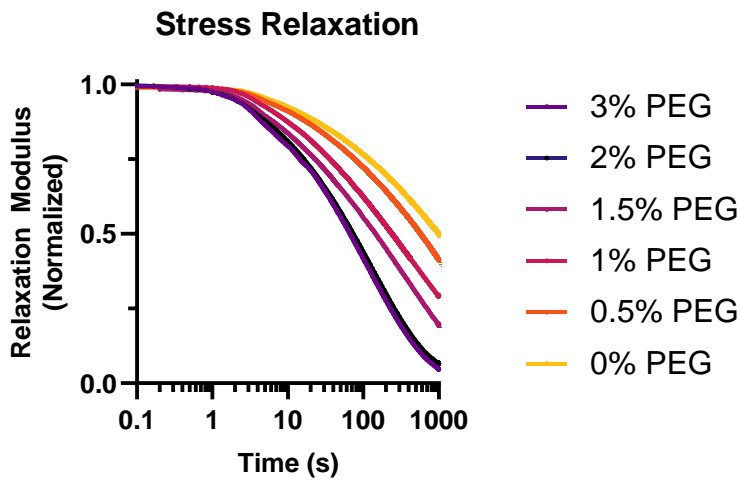


Figure 14 - Stress relaxation plots for 2% norbornene alginate with added PEG. Each group represents an average of N=4.

B.7

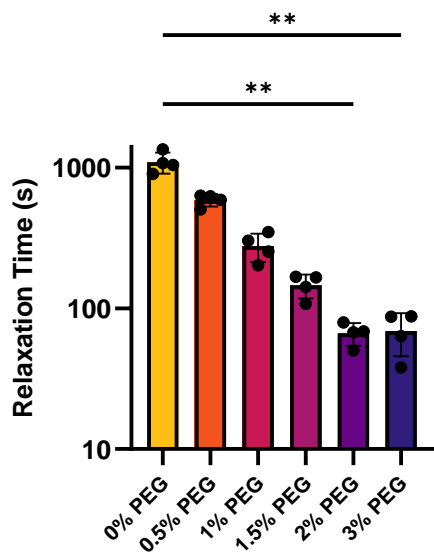


Figure 15 - Relaxation Time ( $\tau_{1/2}$ ) for 2% PEG alginates. Relaxation times were compared using the Kruskal–Wallis analysis of variance, with \*\* indicating  $p < 0.01$ .



## Bibliography

- (1) Streitberger, K.-J.; Reiss-Zimmermann, M.; Freimann, F. B.; Bayerl, S.; Guo, J.; Arlt, F.; Wuerfel, J.; Braun, J.; Hoffmann, K.-T.; Sack, I. High-Resolution Mechanical Imaging of Glioblastoma by Multifrequency Magnetic Resonance Elastography. *PLoS ONE* **2014**, *9* (10), e110588. <https://doi.org/10.1371/journal.pone.0110588>.
- (2) Shahryari, M.; Tzschätzsch, H.; Guo, J.; Marticorena Garcia, S. R.; Böning, G.; Fehrenbach, U.; Stencel, L.; Asbach, P.; Hamm, B.; Käs, J. A.; Braun, J.; Denecke, T.; Sack, I. Tomoelastography Distinguishes Noninvasively between Benign and Malignant Liver Lesions. *Cancer Res.* **2019**, *79* (22), 5704–5710. <https://doi.org/10.1158/0008-5472.CAN-19-2150>.
- (3) Sinkus, R.; Tanter, M.; Xydeas, T.; Catheline, S.; Bercoff, J.; Fink, M. Viscoelastic Shear Properties of in Vivo Breast Lesions Measured by MR Elastography. *Magn. Reson. Imaging* **2005**, *23* (2), 159–165. <https://doi.org/10.1016/j.mri.2004.11.060>.
- (4) Ebihara, T.; Venkatesan, N.; Tanaka, R.; Ludwig, M. S. Changes in Extracellular Matrix and Tissue Viscoelasticity in Bleomycin-Induced Lung Fibrosis. *Am. J. Respir. Crit. Care Med.* **2000**, *162* (4), 1569–1576. <https://doi.org/10.1164/ajrccm.162.4.9912011>.
- (5) Bonnans, C.; Chou, J.; Werb, Z. Remodelling the Extracellular Matrix in Development and Disease. *Nat. Rev. Mol. Cell Biol.* **2014**, *15* (12), 786–801. <https://doi.org/10.1038/nrm3904>.
- (6) Caliani, S. R.; Burdick, J. A. A Practical Guide to Hydrogels for Cell Culture. *Nat. Methods* **2016**, *13* (5), 405–414. <https://doi.org/10.1038/nmeth.3839>.
- (7) Pelham, R. J.; Wang, Y. Cell Locomotion and Focal Adhesions Are Regulated by Substrate Flexibility. *Proc. Natl. Acad. Sci.* **1997**, *94* (25), 13661–13665. <https://doi.org/10.1073/pnas.94.25.13661>.
- (8) Georges, P. C.; Janmey, P. A. Cell Type-Specific Response to Growth on Soft Materials. *J. Appl. Physiol.* **2005**, *98* (4), 1547–1553. <https://doi.org/10.1152/japplphysiol.01121.2004>.
- (9) Peyton, S. R.; Putnam, A. J. Extracellular Matrix Rigidity Governs Smooth Muscle Cell Motility in a Biphasic Fashion. *J. Cell. Physiol.* **2005**, *204* (1), 198–209. <https://doi.org/10.1002/jcp.20274>.
- (10) Yeung, T.; Georges, P. C.; Flanagan, L. A.; Marg, B.; Ortiz, M.; Funaki, M.; Zahir, N.; Ming, W.; Weaver, V.; Janmey, P. A. Effects of Substrate Stiffness on Cell Morphology, Cytoskeletal Structure, and Adhesion. *Cell Motil.* **2005**, *60* (1), 24–34. <https://doi.org/10.1002/cm.20041>.

- (11) Bhana, B.; Iyer, R. K.; Chen, W. L. K.; Zhao, R.; Sider, K. L.; Likhitpanichkul, M.; Simmons, C. A.; Radisic, M. Influence of substrate stiffness on the phenotype of heart cells. *Biotechnol. Bioeng.* **2010**, *105* (6), 1148–1160. <https://doi.org/10.1002/bit.22647>.
- (12) Banerjee, A.; Arha, M.; Choudhary, S.; Ashton, R. S.; Bhatia, S. R.; Schaffer, D. V.; Kane, R. S. The Influence of Hydrogel Modulus on the Proliferation and Differentiation of Encapsulated Neural Stem Cells. *Biomaterials* **2009**, *30* (27), 4695–4699. <https://doi.org/10.1016/j.biomaterials.2009.05.050>.
- (13) Cavo, M.; Fato, M.; Peñuela, L.; Beltrame, F.; Raiteri, R.; Scaglione, S. Microenvironment Complexity and Matrix Stiffness Regulate Breast Cancer Cell Activity in a 3D in Vitro Model. *Sci. Rep.* **2016**, *6* (1), 35367. <https://doi.org/10.1038/srep35367>.
- (14) Rowlands, A. S.; George, P. A.; Cooper-White, J. J. Directing Osteogenic and Myogenic Differentiation of MSCs: Interplay of Stiffness and Adhesive Ligand Presentation. *Am. J. Physiol.-Cell Physiol.* **2008**, *295* (4), C1037–C1044. <https://doi.org/10.1152/ajpcell.67.2008>.
- (15) Vedadghavami, A.; Minooei, F.; Mohammadi, M. H.; Khetani, S.; Rezaei Kolahchi, A.; Mashayekhan, S.; Sanati-Nezhad, A. Manufacturing of Hydrogel Biomaterials with Controlled Mechanical Properties for Tissue Engineering Applications. *Acta Biomater.* **2017**, *62*, 42–63. <https://doi.org/10.1016/j.actbio.2017.07.028>.
- (16) Lee, K. Y.; Mooney, D. J. Alginate: Properties and Biomedical Applications. *Prog. Polym. Sci.* **2012**, *37* (1), 106–126. <https://doi.org/10.1016/j.progpolymsci.2011.06.003>.
- (17) Tibbitt, M. W.; Anseth, K. S. Hydrogels as Extracellular Matrix Mimics for 3D Cell Culture. *Biotechnol. Bioeng.* **2009**, *103* (4), 655–663. <https://doi.org/10.1002/bit.22361>.
- (18) Cao, L.; Lu, W.; Mata, A.; Nishinari, K.; Fang, Y. Egg-Box Model-Based Gelation of Alginate and Pectin: A Review. *Carbohydr. Polym.* **2020**, *242*, 116389. <https://doi.org/10.1016/j.carbpol.2020.116389>.
- (19) Pal, S. Mechanical Properties of Biological Materials. In *Design of Artificial Human Joints & Organs*; Pal, S., Ed.; Springer US: Boston, MA, 2014; pp 23–40. [https://doi.org/10.1007/978-1-4614-6255-2\\_2](https://doi.org/10.1007/978-1-4614-6255-2_2).
- (20) Davis, F. M.; De Vita, R. A Nonlinear Constitutive Model for Stress Relaxation in Ligaments and Tendons. *Ann. Biomed. Eng.* **2012**, *40* (12), 2541–2550. <https://doi.org/10.1007/s10439-012-0596-2>.
- (21) Sarver, J. J.; Robinson, P. S.; Elliott, D. M. Methods for Quasi-Linear Viscoelastic Modeling of Soft Tissue: Application to Incremental Stress-Relaxation Experiments. *J. Biomech. Eng.* **2003**, *125* (5), 754–758. <https://doi.org/10.1115/1.1615247>.

- (22) Nam, S.; Hu, K. H.; Butte, M. J.; Chaudhuri, O. Strain-Enhanced Stress Relaxation Impacts Nonlinear Elasticity in Collagen Gels. *Proc. Natl. Acad. Sci.* **2016**, *113* (20), 5492–5497. <https://doi.org/10.1073/pnas.1523906113>.
- (23) Grashow, J. S.; Sacks, M. S.; Liao, J.; Yoganathan, A. P. Planar Biaxial Creep and Stress Relaxation of the Mitral Valve Anterior Leaflet. *Ann. Biomed. Eng.* **2006**, *34* (10), 1509–1518. <https://doi.org/10.1007/s10439-006-9183-8>.
- (24) Purslow, P. P.; Wess, T. J.; Hukins, D. W. Collagen Orientation and Molecular Spacing during Creep and Stress-Relaxation in Soft Connective Tissues. *J. Exp. Biol.* **1998**, *201* (1), 135–142. <https://doi.org/10.1242/jeb.201.1.135>.
- (25) Chaudhuri, O.; Cooper-White, J.; Janmey, P. A.; Mooney, D. J.; Shenoy, V. B. Effects of Extracellular Matrix Viscoelasticity on Cellular Behaviour. *Nature* **2020**, *584* (7822), 535–546. <https://doi.org/10.1038/s41586-020-2612-2>.
- (26) Sauer, F.; Oswald, L.; Ariza de Schellenberger, A.; Tzschätzsch, H.; Schrank, F.; Fischer, T.; Braun, J.; Mierke, C. T.; Valiullin, R.; Sack, I.; Käs, J. A. Collagen Networks Determine Viscoelastic Properties of Connective Tissues yet Do Not Hinder Diffusion of the Aqueous Solvent. *Soft Matter* **2019**, *15* (14), 3055–3064. <https://doi.org/10.1039/C8SM02264J>.
- (27) Münster, S.; Jawerth, L. M.; Leslie, B. A.; Weitz, J. I.; Fabry, B.; Weitz, D. A. Strain History Dependence of the Nonlinear Stress Response of Fibrin and Collagen Networks. *Proc. Natl. Acad. Sci.* **2013**, *110* (30), 12197–12202. <https://doi.org/10.1073/pnas.1222787110>.
- (28) Yang, W.; Sherman, V. R.; Gludovatz, B.; Schaible, E.; Stewart, P.; Ritchie, R. O.; Meyers, M. A. On the Tear Resistance of Skin. *Nat. Commun.* **2015**, *6*, 6649. <https://doi.org/10.1038/ncomms7649>.
- (29) Ban, E.; Franklin, J. M.; Nam, S.; Smith, L. R.; Wang, H.; Wells, R. G.; Chaudhuri, O.; Liphardt, J. T.; Shenoy, V. B. Mechanisms of Plastic Deformation in Collagen Networks Induced by Cellular Forces. *Biophys. J.* **2018**, *114* (2), 450–461. <https://doi.org/10.1016/j.bpj.2017.11.3739>.
- (30) Brown, A. E. X.; Litvinov, R. I.; Discher, D. E.; Purohit, P. K.; Weisel, J. W. Multiscale Mechanics of Fibrin Polymer: Gel Stretching with Protein Unfolding and Loss of Water. *Science* **2009**, *325* (5941), 741–744. <https://doi.org/10.1126/science.1172484>.
- (31) Oxlund, H.; Manschot, J.; Viidik, A. The Role of Elastin in the Mechanical Properties of Skin. *J. Biomech.* **1988**, *21* (3), 213–218. [https://doi.org/10.1016/0021-9290\(88\)90172-8](https://doi.org/10.1016/0021-9290(88)90172-8).
- (32) Zhao, X. Multi-Scale Multi-Mechanism Design of Tough Hydrogels: Building Dissipation into Stretchy Networks. *Soft Matter* **2014**, *10* (5), 672–687. <https://doi.org/10.1039/c3sm52272e>.

- (33) van Oosten, A. S. G.; Vahabi, M.; Licup, A. J.; Sharma, A.; Galie, P. A.; MacKintosh, F. C.; Janmey, P. A. Uncoupling Shear and Uniaxial Elastic Moduli of Semiflexible Biopolymer Networks: Compression-Softening and Stretch-Stiffening. *Sci. Rep.* **2016**, *6* (1), 19270. <https://doi.org/10.1038/srep19270>.
- (34) Oftadeh, R.; Connizzo, B. K.; Nia, H. T.; Ortiz, C.; Grodzinsky, A. J. Biological Connective Tissues Exhibit Viscoelastic and Poroelastic Behavior at Different Frequency Regimes: Application to Tendon and Skin Biophysics. *Acta Biomater.* **2018**, *70*, 249–259. <https://doi.org/10.1016/j.actbio.2018.01.041>.
- (35) Discher, D. E.; Janmey, P.; Wang, Y.-L. Tissue Cells Feel and Respond to the Stiffness of Their Substrate. *Science* **2005**, *310* (5751), 1139–1143. <https://doi.org/10.1126/science.1116995>.
- (36) DuFort, C. C.; Paszek, M. J.; Weaver, V. M. Balancing Forces: Architectural Control of Mechanotransduction. *Nat. Rev. Mol. Cell Biol.* **2011**, *12* (5), 308–319. <https://doi.org/10.1038/nrm3112>.
- (37) Vogel, V.; Sheetz, M. Local Force and Geometry Sensing Regulate Cell Functions. *Nat. Rev. Mol. Cell Biol.* **2006**, *7* (4), 265–275. <https://doi.org/10.1038/nrm1890>.
- (38) Keese, C. R.; Giaever, I. Substrate Mechanics and Cell Spreading. *Exp. Cell Res.* **1991**, *195* (2), 528–532. [https://doi.org/10.1016/0014-4827\(91\)90406-k](https://doi.org/10.1016/0014-4827(91)90406-k).
- (39) Humphrey, J. D.; Dufresne, E. R.; Schwartz, M. A. Mechanotransduction and Extracellular Matrix Homeostasis. *Nat. Rev. Mol. Cell Biol.* **2014**, *15* (12), 802–812. <https://doi.org/10.1038/nrm3896>.
- (40) Janmey, P. A.; Fletcher, D. A.; Reinhart-King, C. A. Stiffness Sensing by Cells. *Physiol. Rev.* **2020**, *100* (2), 695–724. <https://doi.org/10.1152/physrev.00013.2019>.
- (41) Keating, C. E.; Cullen, D. K. Mechanosensation in Traumatic Brain Injury. *Neurobiol. Dis.* **2021**, *148*, 105210. <https://doi.org/10.1016/j.nbd.2020.105210>.
- (42) Yang, C.; Tibbitt, M. W.; Basta, L.; Anseth, K. S. Mechanical Memory and Dosing Influence Stem Cell Fate. *Nat. Mater.* **2014**, *13* (6), 645–652. <https://doi.org/10.1038/nmat3889>.
- (43) Chaudhuri, O.; Gu, L.; Darnell, M.; Klumpers, D.; Bencherif, S. A.; Weaver, J. C.; Huebsch, N.; Mooney, D. J. Substrate Stress Relaxation Regulates Cell Spreading. *Nat. Commun.* **2015**, *6* (1), 6365. <https://doi.org/10.1038/ncomms7365>.
- (44) Chaudhuri, O.; Gu, L.; Klumpers, D.; Darnell, M.; Bencherif, S. A.; Weaver, J. C.; Huebsch, N.; Lee, H.; Lippens, E.; Duda, G. N.; Mooney, D. J. Hydrogels with Tunable Stress Relaxation Regulate Stem Cell Fate and Activity. *Nat. Mater.* **2016**, *15* (3), 326–334. <https://doi.org/10.1038/nmat4489>.

- (45) McKinnon, D. D.; Domaille, D. W.; Cha, J. N.; Anseth, K. S. Biophysically Defined and Cytocompatible Covalently Adaptable Networks as Viscoelastic 3D Cell Culture Systems. *Adv. Mater.* **2014**, *26* (6), 865–872. <https://doi.org/10.1002/adma.201303680>.
- (47) Malandrino, A.; Trepap, X.; Kamm, R. D.; Mak, M. Dynamic Filopodial Forces Induce Accumulation, Damage, and Plastic Remodeling of 3D Extracellular Matrices. *PLoS Comput. Biol.* **2019**, *15* (4), e1006684. <https://doi.org/10.1371/journal.pcbi.1006684>.
- (48) Liu, A. S.; Wang, H.; Copeland, C. R.; Chen, C. S.; Shenoy, V. B.; Reich, D. H. Matrix Viscoplasticity and Its Shielding by Active Mechanics in Microtissue Models: Experiments and Mathematical Modeling. *Sci. Rep.* **2016**, *6*, 33919. <https://doi.org/10.1038/srep33919>.
- (49) Wisdom, K. M.; Adebawale, K.; Chang, J.; Lee, J. Y.; Nam, S.; Desai, R.; Rossen, N. S.; Rafat, M.; West, R. B.; Hodgson, L.; Chaudhuri, O. Matrix Mechanical Plasticity Regulates Cancer Cell Migration through Confining Microenvironments. *Nat. Commun.* **2018**, *9* (1), 4144. <https://doi.org/10.1038/s41467-018-06641-z>.
- (50) Gupta, V. K.; Chaudhuri, O. Mechanical Regulation of Cell-Cycle Progression and Division. *Trends Cell Biol.* **2022**. <https://doi.org/10.1016/j.tcb.2022.03.010>.
- (51) Lee, H.; Gu, L.; Mooney, D. J.; Levenston, M. E.; Chaudhuri, O. Mechanical Confinement Regulates Cartilage Matrix Formation by Chondrocytes. *Nat. Mater.* **2017**, *16* (12), 1243–1251. <https://doi.org/10.1038/nmat4993>.
- (52) Sinkus, R.; Siegmann, K.; Xydeas, T.; Tanter, M.; Claussen, C.; Fink, M. MR Elastography of Breast Lesions: Understanding the Solid/Liquid Duality Can Improve the Specificity of Contrast-Enhanced MR Mammography. *Magn. Reson. Med.* **2007**, *58* (6), 1135–1144. <https://doi.org/10.1002/mrm.21404>.
- (53) Kloxin, C. J.; Scott, T. F.; Adzima, B. J.; Bowman, C. N. Covalent Adaptable Networks (CANs): A Unique Paradigm in Crosslinked Polymers. *Macromolecules* **2010**, *43* (6), 2643–2653. <https://doi.org/10.1021/ma902596s>.
- (54) Brown, T. E.; Carberry, B. J.; Worrell, B. T.; Dudaryeva, O. Y.; McBride, M. K.; Bowman, C. N.; Anseth, K. S. Photopolymerized Dynamic Hydrogels with Tunable Viscoelastic Properties through Thioester Exchange. *Biomaterials* **2018**, *178*, 496–503. <https://doi.org/10.1016/j.biomaterials.2018.03.060>.
- (55) Zhao, X.; Huebsch, N.; Mooney, D. J.; Suo, Z. Stress-Relaxation Behavior in Gels with Ionic and Covalent Crosslinks. *J. Appl. Phys.* **2010**, *107* (6), 63509. <https://doi.org/10.1063/1.3343265>.
- (56) Dooling, L. J.; Buck, M. E.; Zhang, W.-B.; Tirrell, D. A. Programming Molecular Association and Viscoelastic Behavior in Protein Networks. *Adv. Mater.* **2016**, *28* (23), 4651–4657. <https://doi.org/10.1002/adma.201506216>.

- (57) Mantooh, S. M.; Munoz-Robles, B. G.; Webber, M. J. Dynamic Hydrogels from Host–Guest Supramolecular Interactions. *Macromol. Biosci.* **2019**, *19* (1), 1800281. <https://doi.org/10.1002/mabi.201800281>.
- (58) Highley, C. B.; Rodell, C. B.; Burdick, J. A. Direct 3D Printing of Shear-Thinning Hydrogels into Self-Healing Hydrogels. *Adv. Mater.* **2015**, *27* (34), 5075–5079. <https://doi.org/10.1002/adma.201501234>.
- (59) Dankers, P. Y. W.; Harmsen, M. C.; Brouwer, L. A.; Van Luyn, M. J. A.; Meijer, E. W. A Modular and Supramolecular Approach to Bioactive Scaffolds for Tissue Engineering. *Nat. Mater.* **2005**, *4* (7), 568–574. <https://doi.org/10.1038/nmat1418>.
- (60) Nam, S.; Stowers, R.; Lou, J.; Xia, Y.; Chaudhuri, O. Varying PEG Density to Control Stress Relaxation in Alginate-PEG Hydrogels for 3D Cell Culture Studies. *Biomaterials* **2019**, *200*, 15–24. <https://doi.org/10.1016/j.biomaterials.2019.02.004>.
- (61) Hui, E.; Gimeno, K. I.; Guan, G.; Caliani, S. R. Spatiotemporal Control of Viscoelasticity in Phototunable Hyaluronic Acid Hydrogels. *Biomacromolecules* **2019**, *20* (11), 4126–4134. <https://doi.org/10.1021/acs.biomac.9b00965>.
- (62) Accardo, J. V.; Kalow, J. A. Reversibly Tuning Hydrogel Stiffness through Photocontrolled Dynamic Covalent Crosslinks. *Chem. Sci.* **2018**, *9* (27), 5987–5993. <https://doi.org/10.1039/C8SC02093K>.
- (63) Carberry, B. J.; Rao, V. V.; Anseth, K. S. Phototunable Viscoelasticity in Hydrogels Through Thioester Exchange. *Ann. Biomed. Eng.* **2020**, *48* (7), 2053–2063. <https://doi.org/10.1007/s10439-020-02460-w>.
- (65) Charbonier, F.; Indana, D.; Chaudhuri, O. Tuning Viscoelasticity in Alginate Hydrogels for 3D Cell Culture Studies. *Curr. Protoc.* **2021**, *1* (5), e124. <https://doi.org/10.1002/cpz1.124>.
- (68) Ooi, H. W.; Mota, C.; ten Cate, A. T.; Calore, A.; Moroni, L.; Baker, M. B. Thiol–Ene Alginate Hydrogels as Versatile Bioinks for Bioprinting. *Biomacromolecules* **2018**, *19* (8), 3390–3400. <https://doi.org/10.1021/acs.biomac.8b00696>.
- (69) Grimes, A.; Breslauer, D. N.; Long, M.; Pegan, J.; Lee, L. P.; Khine, M. Shrinky-Dink Microfluidics: Rapid Generation of Deep and Rounded Patterns. *Lab Chip* **2008**, *8* (1), 170–172. <https://doi.org/10.1039/B711622E>.